Japanese Journal of Applied Physics
Vol. 30, No. 5, May, 1991, pp. 1141–1148

# Deformation of Vesicles under the Influence of Strong Electric Fields

Hiroyuki Hyuga, Kazuhiko Kinosita, Jr. and Nobuyoshi Wakabayashi

*Department of Physics, Faculty of Science and Technology, Keio University, Yokohama 223*

(Received January 29, 1991; accepted for publication March 16, 1991)

The deformation of vesicles with conducting membranes in external electric fields has been studied in the framework of the perturbation theory. A simple model for dynamics of deformation is proposed, and the results of numerical calculations for typical combinations of the vesicle size and the electric field are presented. When the conductivity inside a spherical vesicle is larger than that of the exterior medium, the deformations, both static and dynamic, are prolate and, otherwise, they are oblate.

**KEYWORDS:** vesicle deformation, conducting membrane, electric field

## §1. Introduction

During the course of extensive studies on electroporation of cells, the mode of cell deformation in a strong electric field has been observed to depend delicately on the cell environment as well as on the applied field.[1),*] As a model system of cell membranes, phospholipid vesicles may be very suitable for studying essential factors in cell deformations. In his pioneering works on the effects that electric and magnetic fields have on vesicle shape, Helfrich considered various types of strain forces.[2-4)] He concluded that the curvature elastic energy was the most important factor in controlling the nonspherical shapes of vesicles. He also studied the influences of fields on the deformation of lipid bilayers. These studies are concerned with the cases in which the lipid bilayers are perfect insulators. The deformation was found always to be prolate in the static electric field. More recently, Ashe et al. studied the deformation of biological cells having ellipsoidal shapes.[5)] Calculations for various orientations of the cell with respect to the electric field were presented.

Recent microscopic observations demonstrated the formation of aqueous pores in the membranes of liposomes and eggs of sea urchins if they are subjected to very strong electric fields.[1,6)] As a result, the membrane acquires a finite electric conductivity. It was found that the conductivities of the aqueous environment as well as that of the membrane have strong influences on the shape of the vesicle in the field and on the dynamics of the deformation.*

In the present report, we propose a model which takes into account the effects of the finite conductivity, and present the results of calculations of the static as well as dynamic deformations of vesicles. The deformation dynamics of vesicles which have insulating membranes will be discussed elsewhere.

## §2. Electric Forces Acting on Membrane

### 2.1 *Fundamental equations*

We consider the situation in which a vesicle is placed in aqueous solution. The conductivity of the water inside the vesicle is $\sigma_i$ and that of the outside water is $\sigma_e$. In the following, the suffix i (e) is used to designate quantities related to the internal (external) region of the vesicle. The thickness of the membrane is taken to be zero and the electric resistance of the membrane is assumed to be negligible. When the electric field is applied, the fields around the vesicle are determined from the equations

$$\mathrm{div}\,(\sigma_i\,\mathrm{grad}\,\phi_i)=0,\quad \mathrm{div}\,(\sigma_e\,\mathrm{grad}\,\phi_e)=0, \tag{2.1}$$

where $\phi_i$ and $\phi_e$ are the potentials of the inside and outside regions of the vesicle, respectively. Equations (2.1) are derived from the relationship between the electric current and the field, $\boldsymbol{J}=\sigma\boldsymbol{E}$, and the current conservation for a stationary state, $\mathrm{div}\,\boldsymbol{J}=0$, as well as $\boldsymbol{E}=-\mathrm{grad}\,\phi$. Only the cases in which both $\sigma_i$ and $\sigma_e$ are constant are considered so that the equations of (2.1), reduce to

$$\Delta\phi_i=0,\quad \Delta\phi_e=0. \tag{2.2}$$

If we denote the strength of the applied field by $E_0$, the asymptotic form of the potential $\phi_e$ at infinity is

$$\phi_e\to -E_0 z. \tag{2.3}$$

Here the $z$-axis is taken along the direction of the applied field. From rot $\boldsymbol{E}=0$ and div $\boldsymbol{J}=0$, one obtains the following conditions for the potentials on the vesicle surface:

$$\begin{aligned}&\boldsymbol{n}\cdot\mathrm{grad}\,\phi_i=\boldsymbol{n}\cdot\mathrm{grad}\,\phi_e\\ &\sigma_i\boldsymbol{t}\cdot\mathrm{grad}\,\phi_i=\sigma_e\boldsymbol{t}\cdot\mathrm{grad}\,\phi_e.\end{aligned} \tag{2.4}$$

Here the unit vector normal (tangential) to the surface is denoted by $\boldsymbol{n}$ ($\boldsymbol{t}$).

The shape of the vesicle is assumed to be axially symmetric around the $z$-axis and to have a mirror symmetry with respect to a plane perpendicular to the $z$-axis. This plane is taken to be the $x$-$y$ plane. The shape of the vesicle is expressed in the polar coordinates as

$$r=f(\theta) \tag{2.5}$$

and $f(\theta)=f(\pi-\theta)$.

The forces are calculated from the Maxwell stress tensor.[7-9)] In the following, the cgs units will be used. It is then given in terms of the, electric field, $\boldsymbol{E}$, and the dielectric constant, $\varepsilon$, as

$$T_{\alpha\beta}=\frac{\varepsilon}{4\pi}\,(E_\alpha E_\beta-1/2E^2\delta_{\alpha\beta}). \tag{2.6}$$

*H. Itoh and M. Hibino: private communication.

The force per unit area of the vesicle surface is given as

$$F_\alpha=\sum_\beta (T^{(s)}_{e\alpha\beta}-T^{(s)}_{i\alpha\beta})n_\beta, \tag{2.7}$$

where $T^{(s)}_e$ and $T^{(s)}_i$ are the Maxwell tensors evaluated on the surface of the vesicle. $n_\beta$ is the $\beta$-component of the vector $\boldsymbol{n}$. Equations (2.4), (2.6) and (2.7) lead to the expression for the normal component of the force per unit area given as

$$F_n=\frac{\varepsilon_e}{4\pi}\left\{\left[\left(\frac{\sigma_i}{\sigma_e}\right)^2+1-2\frac{\varepsilon_i}{\varepsilon_e}\right](E_{in})^2+\left(\frac{\varepsilon_i}{\varepsilon_e}-1\right)E_i^2\right\}, \tag{2.8}$$

where $E_{in}$ and $E_i$ are, respectively, the normal component and the magnitude of the electric field evaluated on the inner surface of the membrane. The surface charge per unit area $\rho_s$ is determined from the Gauss law as

$$\rho_s=\frac{1}{4\pi}(\varepsilon_e E_{en}-\varepsilon_i E_{in})-\frac{\varepsilon_e}{4\pi}\left(\frac{\sigma_i}{\sigma_e}-\frac{\varepsilon_i}{\varepsilon_e}\right)E_{in}. \tag{2.9}$$

In arriving at the last expression, eq. (2.4) has been used.

One might argue that the force may be derived as a product of the surface charge and a certain linear combination of $E_i$ and $E_e$. However, it is clear from eq. (2.9) that the force of eq. (2.8) would not be given by such a product. This subtle point has been discussed in various text books.[8,9] We use the force given by eq. (2.8) in the present calculation. The tangential component of the electric force should be balanced by the stretching force within the membrane.[4] We assume that this component does not contribute to the force responsible for macroscopic deformation.

### 2.2 *Spherical vesicles*

In the case of a spherical vesicle, the exact solutions of the above equations can be obtained.

The potentlals are given as

$$\phi_e=-E_0\left\{1+\lambda\left(\frac{R}{r}\right)^3\right\}z$$

$$\phi_i=-E_0(1+\lambda)z=-\frac{3\sigma_e}{2\sigma_e+\sigma_i}E_0 z, \tag{2.10}$$

where $R$ is the radius of the vesicle and $\lambda$ is written in terms of the ratio $\sigma_i/\sigma_e$ as

$$\lambda=\frac{1-\sigma_i/\sigma_e}{2+\sigma_i/\sigma_e}. \tag{2.11}$$

Therefore, the electric fields are given as

$$\boldsymbol{E}_e=E_0\left\{1+\lambda\left(\frac{R}{r}\right)^3\right\}\hat{z}-E_0 3\lambda\left(\frac{R}{r}\right)^3\frac{z}{r}\hat{r}$$

$$\boldsymbol{E}_i=E_0(1+\lambda)\hat{z}, \tag{2.12}$$

where $\hat{r}=r/r$ and $\hat{z}=z/r$. The field inside the vesicle turns out to be uniform and is parallel to the applied field. The normal component of the force is expressed as

$$F_n=\frac{9}{8\pi}\cdot\frac{\varepsilon_e E_0^2}{(2+\sigma_i/\sigma_e)}\left\{\left[\left(\frac{\sigma_i}{\sigma_e}\right)^2+1-2\frac{\varepsilon_i}{\varepsilon_e}\right]\cos^2\theta+\frac{\varepsilon_i}{\varepsilon_e}-1\right\}. \tag{2.13}$$

It can be seen from this equation that the deformation is prolate if $(\sigma_i/\sigma_e)^2>2\varepsilon_i/\varepsilon_e-1$ and is oblate otherwise. In the particular case of $\varepsilon_e=\varepsilon_i$, the deformation is prolate if $\sigma_e<\sigma_i$.

### 2.3 *Small deformation*

If the shape of the vesicle is limited to ellipsoids of rotation, the equations can be solved analytically. The expressions for the solutions are given in Appendix A. Analytic solutions for general shapes may be obtained only by a perturbative method. In this subsection, such perturbative solutions are presented.

It is assumed that the deformation is represented as a small deviation from a spherical shape, and the shape is expressed in the form of a multipole expansion given as

$$r=f(\theta)=a(1+g(\theta))$$

and

$$g(\theta)=\sum_{l=1}^{\infty} g_{2l}P_{2l}(\cos\theta), \tag{2.14}$$

where $a$ is a constant and $P_{2l}$'s are the Legendre polynomials. In the following, $g_{2l}$'s are assumed to be small. A convenient measure of deformation is the ratio $r(\theta=0)/r(\theta=\pi/2)$ which is given by

$$\frac{r(\theta=0)}{r(\theta=\pi/2)}=\frac{1+g_2+g_4+\cdots}{1-g_2/2+3g_4/8+\cdots}. \tag{2.15}$$

We denote the radius of the sphere before the application of the field by $a_0$. If the surface area is constant, the difference between $a$ in eq. (2.14) and $a_0$ gives higher-order contributions and is ignored in the following. The potentials $\phi_e$ and $\phi_i$ are expanded as

$$\phi_e=E_0 a_0\left\{-\left[\frac{r}{a_0}+\lambda\left(\frac{a_0}{r}\right)^2\right]\cos\theta+\lambda\sum_{l=0}^{\infty}\phi_e^{(2l+1)}\times\left(\frac{a_0}{r}\right)^{2l+2}P_{2l+1}(\cos\theta)\right\}$$

$$\phi_i=E_0 a_0\left\{-(1+\lambda)\frac{r}{a_0}\cos\theta+\lambda\sum_{l=0}^{\infty}\phi_i^{(2l+1)}\times\left(\frac{r}{a_0}\right)^{2l+1}P_{2l+1}(\cos\theta)\right\}. \tag{2.16}$$

Here the first term on the right-hand side corresponds to the potential for a sphere in the uniform field and the remaining terms represent deviations. In this expression, the effects of mirror symmetry are already taken into account. The perturbative solutions of the coefficients $\phi_e^{(2l+1)}$ and $\phi_i^{(2l+1)}$ are given in Appendix B.

The normal component of the force is expressed as

$$F_n=\sum_{l=0}^{\infty}F^{(2l)}P_{2l}(\cos\theta). \tag{2.16}$$

The explicit forms of coefficients $F^{(2l)}$ are given in Appendix C.

## §3. Deformation in Static Field

The equilibrium shape of a vesicle in electric field has been the subject of various theoretical studies in the past. These studies have treated only the cases in which the lipid bilayers are perfect insulators. We address ourselves to the problems involving bilayers which can be regarded as conductors.

### 3.1 *Balance equations for forces*

According to Helfrich,[2] the elastic energy of a membrane is given by the curvature elastic energy

$$V=\kappa/2\int ds(H-H_0)^2, \tag{3.1}$$

where $\kappa$ is the curvature-elastic modulus, $H$ is the average curvature and $H_0$ is its equilibrium value. The energy associated with the Gaussian curvature is ignored since it makes no contribution in the present problem. We assume that the internal stretching force is so strong that the surface area of the vesicle remains unchanged. This assumption is consistent with the statement made in the previous section about the tangential component of the electric force.

The curvature $H$ for the surface $r=f(\theta)$ is expressed as[10]

$$H=\frac{(2f^2+3f'^2-ff'')f\sin\theta-(f^2+f'^2)f'\cos\theta}{(f^2+f'^2)^{3/2}f\sin\theta}. \tag{3.2}$$

Here $f'=\partial f/\partial\theta$ and $f''=\partial^2 f/\partial\theta^2$.

The equation of motion may be derived by the use of the Lagrangian density $\mathscr{L}$ defined as

$$K-V=\int\mathscr{L}\,d\theta, \tag{3.3}$$

where $K$ is the kinetic energy. In the case of a static problem, $K=0$ and the equation of motion becomes the equation for the force balance

$$\frac{d}{d\theta}\frac{\partial\mathscr{L}}{\partial g'}-\frac{d^2}{d\theta^2}\frac{\partial\mathscr{L}}{\partial g''}-\frac{\partial\mathscr{L}}{\partial g}=aF_n\frac{dS}{d\theta}. \tag{3.4}$$

Here $F_n$ is the electric force per unit area and $dS$ is the surface element given by $dS=2\pi f\sqrt{f^2+f'^2}\sin\theta\,d\theta$.

For small deformations, $V$ is written in terms of $g$ of eq. (2.14) as

$$V=8\pi\kappa\int\sin\theta\,d\theta\left\{\frac{1}{8}(g''-g'\cos\theta)^2+\frac{1}{2}g^2-\frac{1}{4}g'^2\right\}. \tag{3.5}$$

In deriving eq. (3.5), use has been made of the condition that the surface area remains constant. The final form of the balance equation turns out to be

$$\frac{4\kappa}{a_0}(l+1)^2(2l+1)^2 g_{2l}=F_{\mathrm{eff}}^{(2l)}. \tag{3.6}$$

The explicit form of $F_{\mathrm{eff}}^{(2l)}$ is given in Appendix C.

### 3.2 *Equilibrium shape*

In this subsection, eq. (3.6) is used to discuss the conditions for the existence of equilibrium shape. The coefficient $F_{\mathrm{eff}}^{(2l)}$ contains contributions from $g_{2l}$, $g_{2l-2}$ and $g_{2l+2}$. As can be seen easily from eq. (3.6) and Appendix C, $g_{2l}$ is proportional to $E^{2l}$. Thus, for a relatively weak field, the term involving $g_{2l+2}$ in $F_{\mathrm{eff}}^{(2l)}$ may be ignored. It should be noted that the equilibrium shape is attained only when the field is rather weak. Since the quadrupole deformation is dominant in the present situation, we first discuss this type of deformation. Equation (3.6) then reduces to

$$C_2 g_2=J \tag{3.7}$$

where

$$J=a_0^2\varepsilon_e E_0^2\frac{3}{4\pi}\frac{x^2-1}{(x+2)^2} \tag{3.8}$$

$$C_2=144\frac{\kappa}{a_0}-J\frac{109x-34}{35(x+2)} \tag{3.9}$$

and $x=\sigma_i/\sigma_e$, and $\varepsilon_i$ is taken to be equal to $\varepsilon_e$.

By defining the quantity $E_\kappa$ as

$$E_\kappa=\sqrt{\frac{26880}{17}\cdot\frac{\kappa}{a_0^3}}, \tag{3.10}$$

eq. (3.9) can be written as

$$C_2=\frac{144}{a_0}\left[1-\frac{\varepsilon_e E_0^2}{E_\kappa^2}\frac{4(x^2-1)(109x-34)}{17(x+2)^3}\right]. \tag{3.11}$$

As a function of $x$ and $\sqrt{\varepsilon_e}E_0/E_\kappa$, $g_2$ can be given by the expression

$$g_2=-\frac{140(x^2-1)(x+2)}{17(x+2)^3\frac{1}{\varepsilon_e}\left(\frac{E_\kappa}{E_0}\right)^2-4(x^2-1)(109x-34)}. \tag{3.12}$$

It will be shown in the next section that, in order for an equilibrium shape to exist, the coefficient $C_2$ must be positive. For $34/109<x<1$, $C_2$ is positive so that an oblate equilibrium shape always exists. For $x>1$ or $x<34/109$, an equilibrium shape can exist only if the electric field $E_0$ satisfies the condition

$$E_0<E_0(|g_2|=\infty)=E_\kappa\left[\frac{17(x+2)^3}{\varepsilon_e 4(x^2-1)(109x-34)}\right]^{1/2}. \tag{3.13}$$

The shape is prolate for $x>1$ and oblate for $x<34/109$. The ratio, $\sqrt{\varepsilon_e}E_0/E_\kappa$, for $|g_2|=\infty$ is plotted against $x$ in Fig. 1.

The above argument is based on the linearized expressions, and the conditions derived therefrom are certainly unsatisfactory. In order to find more realistic conditions, we need to go beyond the present degree of perturbation. However, in estimating the field strength, $E_0$, for which an equilibrium shape exists, we will be satisfied by merely requiring that $|g_2|$ remains less than a certain small value. Figure 1 also shows the ratios, $\sqrt{\varepsilon_e}E_0/E_\kappa$, for $|g_2|=1/2$ and $1/4$. It should be noted that $\sqrt{\varepsilon_e}E_0$ is of the same order of magnitude as $E_\kappa$ as long as $\sigma_i/\sigma_e$ is not very close to unity. Since $E_\kappa$ is inversely proportional to $a_0^{3/2}$, a small vesicle can have an equilibrium shape even for a rather large external field.

For a vesicle having the radius of 10 $\mu$m and $\kappa=5\times10^{-13}$ erg,[2,3] $E_\kappa$ is 472 V·cm$^{-1}$. If the fluids both inside and outside this vesicle are water ($\varepsilon_e=81$) and the conductivity ratio, $x$, is 0.5, $E_0(|g_2|=1/2)$ is 40 V·cm$^{-1}$. For $x=2.0$, $E_0(|g_2|=1/2)$ is 23 V·cm$^{-1}$.

It can be shown that $g_4$ associated with the octapole deformation is given as

$$g_4=\frac{108}{35}\left(\frac{C_4}{C_2}\right)(g_2)^2 \tag{3.14}$$

where

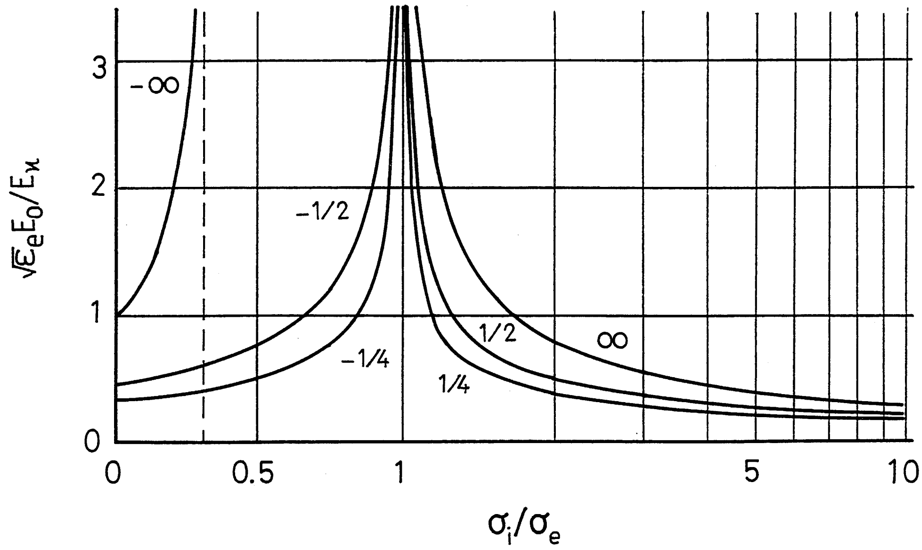


Fig. 1. $\sqrt{\varepsilon_e}E_0/E_\kappa$ vs $\sigma_i/\sigma_e$ for various values of $g_2$ as indicated. Note that a linear scale is used for $0<\sigma_i/\sigma_e<1$, whereas the scale is logarithmic for $\sigma_i/\sigma_e>1$. The broken line corresponds to $\sigma_i/\sigma_e=34/109$.

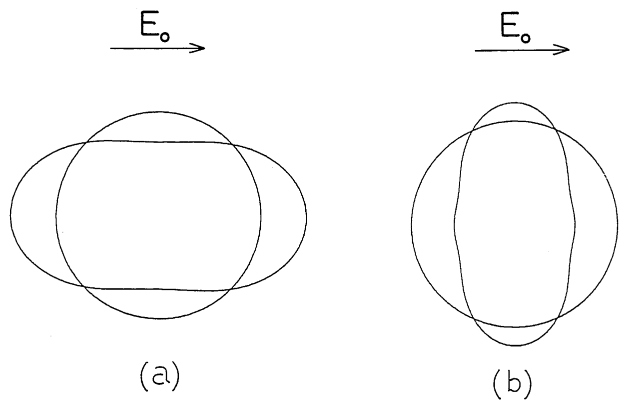


Fig. 2. Shapes of vesicles (a) for $x=2$ and $g_2=1/2$ ($g_4=0.084$) and (b) for $x=1/2$ and $g_2=-1/2$ ($g_4=0.149$).

$$C_4=\frac{900\kappa}{a_0}-J\frac{1403x-1004}{77(3x+4)}. \tag{3.15}$$

For a finite $g_2$, $C_2/C_4$ can be shown to be positive and, hence, $g_4$ is positive. Figure 2 shows the shapes of vesicles for $x=1/2$ and $g_2=-1/2$ ($g_4=0.149$) as well as for $x=2$ and $g_2=1/2$ ($g_4=0.084$).

## §4. Model of Dynamics

The electric fields used in some of the experiments such as that of Itoh *et al.*[1)] and Kinosita *et al.*[6)] are fairly strong so that the vesicles were ruptured if the fields were kept for sufficiently long times. Therefore, the equilibrium shape will not be attained in such cases. When pulse fields were utilized, the vesicles were found to undergo deformation without being ruptured and exhibit relaxational phenomena after the fields were switched off. We propose a simple model which describes the time variation of the vesicle shape.

### 4.1 *Equations of motion*

The model is based on the assumptions that the vesicle is initially spherical and that the deformation is small. In addition, it is assumed that the electric field is adiabatically determined by the equations given in §2.

The dynamical deformation of the vesicle is closely coupled with the motions of fluid surrounding the membrane. For a satisfactory description of the dynamics, complex hydrodynamical calculations are required. In the present discussion, we simply assume that the equation for the fluid motion consists of the inertial term and the term corresponding to the resistance of the fluid. The forces associated with the elastic as well as Maxwell stresses are included in the equation. The inertial term represents the mass of the fluid which is forced to move by the motion of the membrane. The kinetic energy is then given by

$$K=\int\frac{1}{2}\rho_m v_n^2\,dS=\int\rho_m\frac{f^3\dot{f}^2}{\sqrt{f^2+f'^2}}\pi\sin\theta\,d\theta, \tag{4.1}$$

if only the fluid motion normal to the surface is assumed to contribute to the inertial term. Here $\rho_m$ is the effective mass per unit area, $v_n$ is the normal component of the velocity of the surface and the dot designates the time derivative. $\rho_m$ is not the mass per unit area of the membrane but includes the mass of the fluid forced to move by the membrane as mentioned above.

For small deviations, one obtains

$$K=\pi a_0^4\int\rho_m\dot{g}^2\sin\theta\,d\theta$$
$$=2\pi\rho_m a_0^4\sum_{l=1}^{\infty}\frac{1}{4l+1}(\dot{g}_{2l})^2. \tag{4.2}$$

$\rho_m$ is taken to be constant. The equation of motion is derived from the Lagrangian density eq. (3.4) and given as

$$\frac{d}{dt}\frac{\partial\mathscr{L}}{\partial\dot{g}}+\frac{d}{d\theta}\frac{\partial\mathscr{L}}{\partial g'}-\frac{d^2}{d\theta^2}\frac{\partial\mathscr{L}}{\partial g''}-\frac{\partial\mathscr{L}}{\partial g}$$
$$=-\gamma a_0 v_n\frac{dS}{d\theta}+a_0F_n\frac{dS}{d\theta}, \tag{4.3}$$

where the first term on the right-hand side represents the effect of the fluid resistance which is assumed to be proportional to the volume swept by the surface in unit time. The inertial and resistance terms in eq. (4.3) add two terms to the balance equation, eq. (3.6), and the resulting equation of motion in the perturbative treatment is

$$\rho_m a_0^3 \ddot{g}_{2l} + \gamma a_0^3 \dot{g}_{2l} + \frac{4\kappa}{a_0}(l+1)^2(2l+1)^2 g_{2l} = F_{\text{eff}}^{(2l)}. \tag{4.4}$$

### 4.2 *Analytic solutions and numerical analysis*

Within the approximation employed in the static case, the final dynamical equations turn out to be simple coupled linear differential equations given by

$$\rho_m a_0^3 \ddot{g}_{2l} + \gamma a_0^3 \dot{g}_{2l} + C_{2l} g_{2l} = \frac{6l(2l-1)^2}{(4l-3)(4l-1)} J g_{2l-2} \tag{4.5}$$

with $g_0 = 1/2$. The quantities $J$, $C_2$ and $C_4$ are defined in §3.2.

After the electric field is switched off, the terms involving the electric field in eq. (4.5) vanish and the dynamical equations become those of uncoupled damped harmonic oscillators. It can be seen that, if $C_2$ is negative, the deformation becomes unbound and the equilibrium shape does not exist. This is the basis for the discussion of §3.2. We introduce the mass factor, $\nu$, as the ratio of the total effective inertial mass to the mass of the fluid inside the vesicle. Then $\mu_m$ is related to $\nu$ as

$$\rho_m 4\pi a_0^2 = \frac{4\pi}{3}\rho_w a_0^3 \nu, \tag{4.6}$$

where $\rho_w$ is the mass per unit volume of the fluid.

Equations for $g_2$ and $g_4$ are obtained from eqs. (4.5) and (4.6) as

$$\ddot{g}_2 + 2\Gamma\dot{g}_2 + D_2 g_2 = 2G \tag{4.7}$$

$$\ddot{g}_4 + 2\Gamma\dot{g}_4 + D_4 g_4 = \frac{216}{35} G g_2 \tag{4.8}$$

where

$$\Gamma = \frac{3\gamma}{\nu\rho_w a_0}. \tag{4.9}$$

By defining $K_2$, $K_4$ and $K_E$ as

$$K_2 = \frac{432\kappa}{\nu\rho_w a_0^5}, \quad K_4 = \frac{25}{4}K_2 \tag{4.10}$$

and

$$K_E = \frac{9\varepsilon_e E_0^2}{8\pi\nu a_0^2 \rho_w}, \tag{4.11}$$

other coefficients in eqs. (4.7) and (4.8) are expressed as

$$D_2 = K_2 - K_E \frac{2(x^2-1)(109x-34)}{35(x+2)}, \tag{4.12}$$

$$D_4 = K_4 - K_E \frac{2(1403x-1004)}{77(3x+4)}, \tag{4.13}$$

and

$$G = K_E \frac{x^2-1}{(x+2)^2}. \tag{4.14}$$

We now solve these equations for a pulse field having the amplitude of $E_0$ and the duration of $t_0$. The vesicle is initially a sphere of radius $a_0$. One can easily obtain the exact solution of eq. (4.7) as

$$g_2 = \frac{2G}{D_2}\left[1 - e^{-\Gamma t}C(\beta t) - \frac{\Gamma}{\beta}e^{-\Gamma t}S(\beta t)\right], \tag{4.15}$$

where $\beta = \sqrt{|\Gamma^2 - D_2|}$. The functions $C(x) = \cosh(x)$ and $S(x) = \sinh(x)$ for $\Gamma^2 > D_2$ while $C(x) = \cos(x)$ and $S(x) = \sin(x)$ for $\Gamma^2 < D_2$. As long as $t_0$ is not large, the third term in the right-hand side of eq. (4.7) has a negligible effect on the dynamics. In particular, eq. (4.15) at $t = t_0$ reduces to

$$g_2(t_0) = \frac{Gt_0}{\Gamma}\left\{1 + \frac{e^{-2\Gamma t_0} - 1}{2\Gamma t_0}\right\}. \tag{4.16}$$

Since $\Gamma t_0 \propto (t_0/a_0)$ and $Gt_0/\Gamma \propto E_0^2(t_0/a_0)$, the deformation at $t_0$ is proportional to $E_0^2$. Furthermore, with a fixed value of $E_0$, the degree of the deviation from a sphere, $g_2(t_0)$, is a function of only $t_0/a_0$.

The equations determining $g_2$ and $g_4$ after the field is turned off are obtained from eqs. (4.7) and (4.8) by setting $K_E = 0$. They are

$$\ddot{g}_2 + 2\Gamma\dot{g}_2 + K_2 g_2 = 0 \tag{4.17}$$

$$\ddot{g}_4 + 2\Gamma\dot{g}_4 + K_4 g_4 = 0. \tag{4.18}$$

Equations (4.17) and (4.18) are solved under the condition that $g_2$ and $g_4$ connect smoothly with the solutions at $t = t_0$ (eq. (4.16)) and a similar expression for $g_4(t_0)$. The result for $g_2$ is

$$g_2 = e^{-\Gamma\tau}\left\{g_2(t_0)C(\alpha\tau) + \frac{1}{\alpha}(\dot{g}_2(t_0) + \Gamma g_2(t_0))S(\alpha\tau)\right\}, \tag{4.19}$$

where $\alpha = \sqrt{|\Gamma^2 - K_2|}$ and $\tau = t - t_0$. The function $g_2$ continues to increase after the field is turned off but eventually exhibits either a relaxational time variation or a damped oscillation, depending on $\Gamma^2 - K_2 > 0$ or $< 0$.

The maximum of $g_2$ occurs at time $t_{max}$ which satisfies the equation

$$\frac{S(\alpha(t_{max} - t))}{C(\alpha(t_{max} - t))} = \frac{\alpha\dot{g}_2(t_0)}{\Gamma\dot{g}_2(t_0) + K_2 g_2(t_0)}. \tag{4.20}$$

The value of $g_2$ at $t_{max}$ may be expressed as

$$g_2(t_{max}) = g_2(t_0)\, e^{-\Gamma(t_{max} - t_0)} \times \sqrt{1 + \frac{2\Gamma\dot{g}_2(t_0)}{K_2 g_2(t_0)} + \frac{1}{K_2}\left(\frac{\dot{g}_2(t_0)}{g_2(t_0)}\right)^2}. \tag{4.21}$$

The relaxation time, $t_r$, is equal to $1/\Gamma$ for the damped oscillation and $t_r = (\Gamma + \alpha)/K_2$ for the exponential damping. In particular, for the critical damping, the relaxation time is $1/\sqrt{K_2}$.

Equations (4.9) and (4.10) for $g_4$ have been solved analytically, but the explicit expressions are somewhat cumbersome and will not be given.

Numerical calculations of $g_2$ and $g_4$ have been carried out for a typical set of values of $E_0 = 500\ \text{V}\cdot\text{cm}^{-1}$, $a_0 = 10$ μm and $t_0 = 500$ μs.[1] The conditions for perturbative calculations are satisfied for this set of values. Figures 3 and 4 show the calculated time developments of deformation. Also shown are the results of calculation for $E_0=500\ \mathrm{V\cdot cm^{-1}}$, $a_0=100\ \mu\mathrm{m}$ and $t_0=5000\ \mu\mathrm{s}$. Since the values for $\gamma$ and $\nu$ are not well established, $\gamma=7.5\ \mathrm{g\cdot cm^{-2}s^{-1}}$, one-half the Stokes resistance force, and $\nu=10$ were used. Calculations were performed using exact solutions. Since $g_2$ and $g_4$ for $0<t<t_0$ in the figures are indistinguishable for two quite different values of $a_0$ if $a_0/t_0$ is the same, one can conclude that the approximate expression for $g_2(t_0)$, eq. (4.16), and a similar expression for $g_4(t_0)$ are adequate and that the perturbation approach is valid. In the approximation of small $t_0$, $g_2(t_{max})/g_2(t_0)$ is a function of $t_0/a_0$ and independent of $E_0$. It can be seen from eqs. (4.20) and (4.21) that the ratio $g_2(t_{max})/g_2(t_0)$ is determined by $t_0/a_0$. Since the calculations of Figs. 3 and 4 were carried out with $t_0/a_0$ held fixed, $g_2(t_{max})/g_2(t_0)$ is the same for all the values of $a_0$. For $t>t_{max}$, the time variation is given by the exponential damping, nearly independent of $a_0$. One can see that $g_4$ damps out more rapidly than $g_2$. In the present case, the relaxation time of $g_4$ is approximately $4/25$ times that of $g_2$. One expects that, for $x>1$, both $g_2$ and $g_4$ are always positive as shown in Fig. 3 for $x=2$. For $x<1$, $g_2$ is always negative while $g_4$ is always positive as exemplified by Fig. 4 for $x=0.2$.

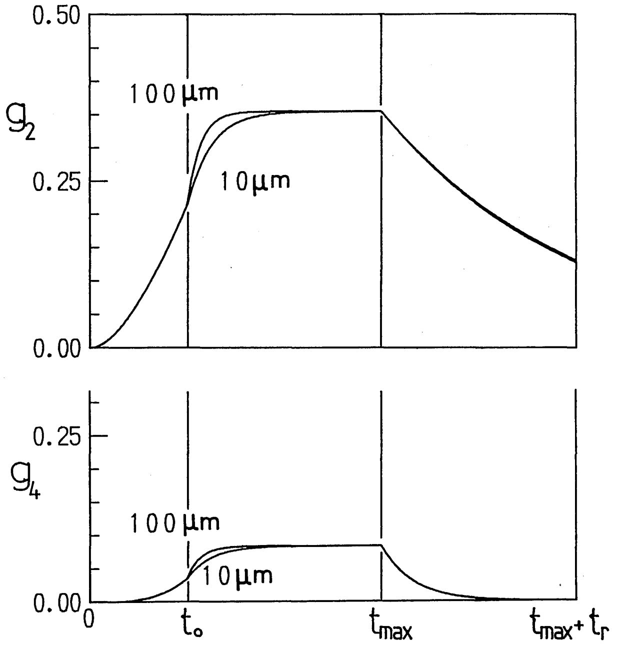


Fig. 3. Time developments of $g_2$ and $g_4$ calculated for $x=2$. The calculations were performed for $a_0=10$ and $100\ \mu\mathrm{m}$ with the constraint $a_0/t_0=10\ \mu\mathrm{m}/500\ \mu\mathrm{s}$. $E_0$ is fixed at $500\ \mathrm{V\cdot cm^{-1}}$ in the calculations. The linear scales for the regions $0<t<t_0$, $t_0<t<t_{max}$ and $t_{max}<t<t_{max}+t_r$ are different and depend strongly on $a_0$. The definitions and values of $t_0$, $t_{max}$ and $t_r$ are given in the text.

It should be noted that the actual values of $t_{max}$ and $t_r$ are quite dependent on the values of $a_0$. For example, $t_{max}$ and $t_r$ for $a_0=10\ \mu\mathrm{m}$ are $3.58t_0$ and $21.5t_0$, respectively, while the corresponding values for $a_0=100\ \mu\mathrm{m}$ are $t_{max}=6.51t_0$ and $t_r=21500t_0$. It can be shown that $t_r$ is proportional to $a_0$ in the limit of large resistance force.

The effect of resistance force is shown in Fig. 5. The curve 1 is the same as that in Fig. 3 and represents the result of the calculation for $E_0=500\ \mathrm{V\cdot cm^{-1}}$, $t_0=500\ \mu\mathrm{s}$, $a_0=10\ \mu\mathrm{m}$ and $\gamma=7.5\ \mathrm{g\cdot cm^{-2}s^{-1}}$. The curves 2 and 3 correspond to the calculations for $\gamma$ twice and three times that of curve 1, respectively. As expected, $g_2(t_0)$ depends strongly on the resistance force. It is interesting to note

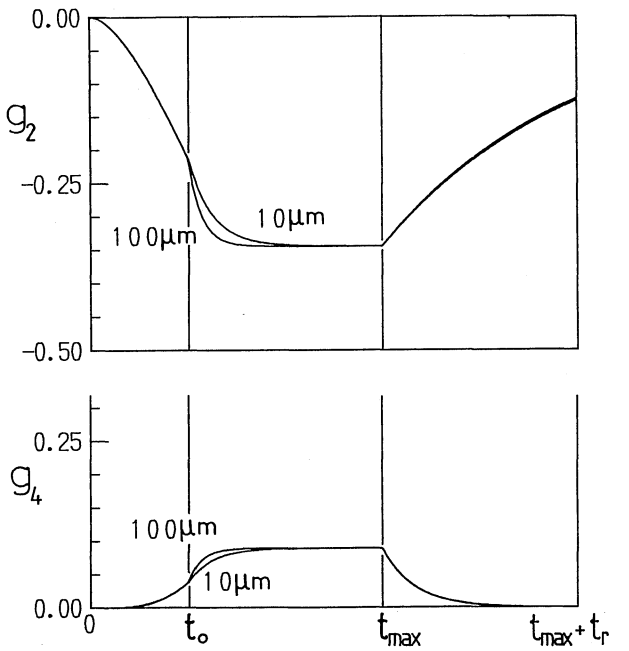


Fig. 4. Time developments of $g_2$ and $g_4$ calculated for $x=0.2$. The calculations were performed for $a_0=10$ and $100\ \mu\mathrm{m}$ with the constraint $a_0/t_0=10\ \mu\mathrm{m}/500\ \mu\mathrm{s}$. $E_0$ is fixed at $500\ \mathrm{V\cdot cm^{-1}}$ in the calculations. The linear scales for the regions $0<t<t_0$, $t_0<t<t_{max}$ and $t_{max}<t<t_{max}+t_r$ are different and depend strongly on $a_0$. The definitions and values of $t_0$, $t_{max}$ and $t_r$ are given in the text.

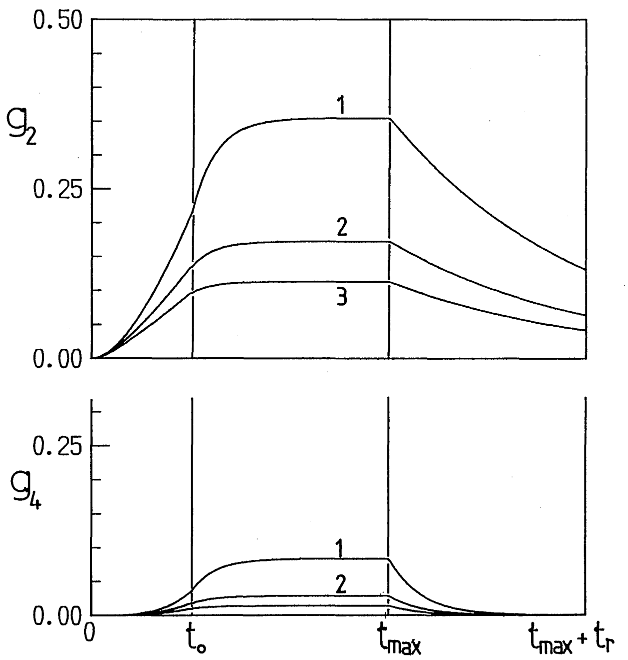


Fig. 5. Effects of resistance on time developments of $g_2$ and $g_4$ for $x=2$. Calculations were performed for $E_0=500\ \mathrm{V\cdot cm^{-1}}$, $t_0=500\ \mu\mathrm{s}$ and $a_0=10\ \mu\mathrm{m}$. Curves 1, 2 and 3 correspond to the calculations with $\gamma=7.5$, 15 and $22.5\ \mathrm{g\cdot cm^{-2}s^{-1}}$, respectively. Curve 1 is also shown in Fig. 3.

that the dependence of $g_2(t_{max})/g_2(t_0)$ on $\gamma$ is much more pronounced.

In the calculations described above, the mass factor, $\nu$, was assumed to be 10. In order to study the dependence of the time development of deformation on this factor, calculations were carried out for various values of $\nu$. It was found that $(t_{max}-t_0)/t_0$ is approximately proportional to $\nu$. For example, in the case of $x=2$, $(t_{max}-t_0)/t_0$ is 3.57 for $\nu=10$, 1.10 for $\nu=3$ and 0.37 for $\nu=1$. The maximum deformation, $g_2(t_{max})$, depends relatively weakly on $\nu$, but $g_2(t_0)$ and therefore $g_2(t_{max})/g_2(t_0)$ depend sensitively on $\nu$. On the other hand, the relaxation time, $t_r$, is hardly affected by the choice of the value for $\nu$.

## §5. Conclusions

The deformation of vesicles with conducting membranes under the influence of electric fields has been shown to critically depend on the relative values of the conductivities inside and outside the vesicle. When the field is weak, the static equilibrium shapes could be calculated by a perturbative method. If the field is strong, this type of calculation is useful when the field is applied only for a short time. Although vesicles usually have insulating membranes, they were assumed to become conducting immediately after a strong field is applied. If the membrane remains insulating for a finite period of time, the present theory needs modifications. Calculations based on such modifications are being performed and will be reported elsewhere.

**Acknowledgements**

We thank Messrs. M. Itoh and M. Hibino for communicating with us concerning unpublished data on vesicle deformations. We also thank Profs. Y. Saito and R. Fukuda for their continued interest and encouragement throughout the present study.

## Appendix A: Solutions for an Ellipsoid of Rotation

Spheroidal coordinates are denoted as $\xi$, $\eta$, and $\zeta$. They are related to the Cartesian coordinates in the following way:

$$z=c\xi\eta,\quad \rho=\sqrt{x^2+y^2}=c\sqrt{(\xi^2\mp1)(1-\eta^2)}$$
$$x=\rho\cos(\varphi),\quad y=\rho\sin(\varphi), \tag{A·1}$$

where the upper (lower) sign in $\rho$ corresponds to the prolate (oblate) spheroidal coordinates, and $c$ is a parameter to be chosen.

The surface of a vesicle is assumed to be specified in the Cartesian coordinates as

$$\frac{z^2}{a^2}+\frac{x^2+y^2}{b^2}=1. \tag{A·2}$$

Then, by defining $c=\sqrt{|b^2-a^2|}$, the surface is given in the spheroidal coordinates simply as

$$\xi=\frac{a}{c}=\xi_0, \tag{A·3}$$

In this case, solutions for eq. (2.2) with the boundary conditions (2.3) and (2.4) are easily obtained. They are expressed as

$$\phi_e=-E_0c[\xi+AF(\xi)]$$
$$\phi_i=-E_0Bc\xi\eta=-E_0Bz, \tag{A·4}$$

where the coefficients $A$ and $B$ are given as

$$A=\frac{(\sigma_e-\sigma_i)\xi_0}{\sigma_iF(\xi_0)-\sigma_e\xi_0F'(\xi_0)}$$

and

$$B=\frac{\sigma_e[F(\xi_0)-\xi_0F'(\xi_0)]}{\sigma_iF(\xi_0)-\sigma_e\xi_0F'(\xi_0)} \tag{A·5}$$

Furthermore, the functions $F(\xi)$ and $F'(\xi)$ are related to the Legendre function of the second kind of the order one $Q_1(\xi)$ as

$$F(\xi)=Q_1(\xi),\quad F'(\xi)=\frac{d}{d\xi}Q_1(\xi)$$

for prolate and

$$F(\xi)=Q_1(i\,\xi),\quad F'(\xi)=\frac{d}{d\xi}Q_1(i\,\xi)$$

for oblate.

We note that the electric field inside the vesicle is parallel to the applied field and is constant.

The normal component of the force per unit area, eq. (2.8), is expressed as

$$F_n=\frac{\varepsilon_e}{8\pi}E_0^2B^2\left\{(\xi^2\mp1)\left[\left(\frac{\sigma_i}{\sigma_e}\right)^2+1-2\left(\frac{\varepsilon_i}{\varepsilon_e}\right)\right]\right.$$
$$\left.\times\frac{\eta^2}{\xi_0^2\mp\eta^2}+\frac{\varepsilon_i}{\varepsilon_e}-1\right\}, \tag{A·6}$$

where the upper (lower) sign corresponds to the prolate (oblate) shape. The area element $dS$ is $2\pi ab[1-(1-b^2/a^2)\eta^2]^{1/2}\,d\eta$. Since the possible range of the values $\xi_0$ is $\xi_0>1$ for a prolate case and $\xi_0>0$ for an oblate case and $-1\leq\eta\leq1$, it is always satisfied that $\xi_0^2\mp1>0$ and $\xi_0^2\mp\eta^2>0$. Therefore, the force induces prolate deformation if $(\sigma_i/\sigma_e)^2>2(\varepsilon_i/\varepsilon_e)-1$ and oblate deformation otherwise. This result is the same as that in the case of a sphere.

## Appendix B: Coefficients $\phi_e^{(2l+1)}$ and $\phi_i^{(2l+1)}$ in eq. (2.16)

To the first order in $g_{2l}$, these coeffcients are shown to be

$$\phi_e^{(2l+1)}=-\frac{3(2l+1)}{4l+1}g_{2l}+\frac{3(2l+1)(\sigma_e-\sigma_i)}{(2l+2)\sigma_e+(2l+1)\sigma_i}\cdot\frac{2l+2}{4l+5}g_{2l+2}$$

and

$$\phi_i^{(2l+1)}=\frac{3(2l+2)\sigma_e}{(2l+2)\sigma_e+(2l+1)\sigma_i}\cdot\frac{(2l+2)(4l+3)}{4l+5}g_{2l+2}.$$

## Appendix C: Coefficients $F^{(2l)}$ in eq. (2.17) and $F_{eff}^{(2l)}$ in eqs. (3.6) and (4.4)

Up to the first order in $g_{2l}$, $F^{(2l)}$ is given as

$$F^{(2l)}=\frac{9\varepsilon_e}{8\pi}E_0^2\frac{1}{(2+\sigma_i/\sigma_e)^2}\left\{\left(\frac{\zeta}{3}+\frac{\varepsilon_i}{\varepsilon_e}-1\right)\delta_{l0}+\frac{2}{3}\eta\delta_{l1}\right.$$
$$+2\zeta\left[\frac{(2l-2)(2l-1)}{(4l-3)(4l-1)}g_{2l-2}-\frac{2l(2l+1)}{(4l-1)(4l+3)}g_{2l}\right.$$

$$
-\frac{(2l+1)(2l+2)(2l+3)}{(4l+3)(4l+5)}g_{2l+2}\Bigg]
-2\zeta\frac{\sigma_e-\sigma_i}{3\sigma_e}\left[\frac{(2l-1)2l}{4l-1}\phi_i^{(2l-1)}+\frac{(2l+1)^2}{4l+3}\phi_i^{(2l+1)}\right]
-\left(\frac{\varepsilon_i}{\varepsilon_e}-1\right)\frac{\sigma_e-\sigma_i}{3\sigma_e}(2l+1)\phi_i^{(2l+1)}\Bigg\}.
$$

Here we defined

$$\zeta=(\sigma_i/\sigma_e)^2+1-2(\varepsilon_i/\varepsilon_e).$$

The force in eq. (4.3) is a product of $F_n$ and $dS/d\theta$. Including the dependence of $dS$ on $g$, we define

$$F_{eff}2\pi a_0\sin\theta\,d\theta=aF_n\frac{dS}{d\theta}d\theta=aF_n2\pi f\sqrt{f^2+f'^2}\sin\theta\,d\theta.$$

Up to the order of $g$, $F_{eff}$ is simply given as

$$F_{eff}=F_n+2g(\theta)F_n.$$

Then, the coefficients $F_{eff}$ in the multipole expansion

$$F_{eff}=\sum F_{eff}^{(2l)}P_{2l}(\cos\theta)$$

are given as

$$
F_{eff}^{(2l)}=F^{(2l)}+\frac{9\varepsilon_eE_0^2}{8\pi}\cdot\frac{1}{(2+\sigma_i/\sigma_e)^2}\left\{2\left(\frac{\varepsilon_i}{\varepsilon_e}-1\right)g_{2l}
+2\zeta\left[\frac{(2l-1)2l}{(4l-3)(4l-1)}g_{2l-2}+\frac{8l^2+4l-1}{(4l-1)(4l+3)}g_{2l}
+\frac{(2l+1)(2l+2)}{(4l+3)(4l+5)}g_{2l+2}\right]\right\}.
$$

## References


1) H. Itoh, M. Hibino, M. Shigemori, M. Koishi, A. Takahashi, T. Hayakawa and K. Kinosita, Jr.: *Proc. SPIE* **1204** (1990) 49.
2) W. Helfrich: Z. Naturforsch. **28c** (1973) 693.
3) W. Helfrich: Phys. Lett. **43A** (1973) 409.
4) W. Helfrich: Z. Naturforsch. **29c** (1974) 182.
5) J. W. Ashe, D. K. Bogen and S. Takashima: Ferroelectrics **86** (1988) 311.
6) K. Kinosita, Jr., I. Ashikawa, N. Saita, H. Yoshimura, H. Itoh, K. Nagayama and A. Ikegami: Biophys. J. **53** (1988) 1015.
7) R. S. Allan and S. G. Mason: Proc. Royal. Soc. **A267** (1962) 45.
8) J. A. Stratton: *Electromagnetic Theory* (McGraw-Hill, New York, 1940).
9) L. D. Landau and E. M. Lifshitz: *Electrodynamics of Continuous Media* (Pergamon, London, 1960).
10) See, for example, J. J. Stoker: *Differential Geometry* (Wiley-Interscience, New York, 1969).